mathematics

MDPI

Article

Thermal-Diffusive Processes of an Electron-Hole Non-Local Semiconductor Model with Variable Thermal Conductivity and Hall Current Effect

Abeer Alhashash [1], Merfat H. Raddadi [2], Alaa A. El-Bary [3,4], Riadh Chteoui [5,6], Abdelwaheb Mhemdi [7,*] and Khaled Lotfy [8,*]

[1] Department of Mathematics, College of Science, Jouf University, P.O. Box 2014, Sakaka 24241, Saudi Arabia
[2] Department of Mathematics, Faculty of Science, Taibah University, Madinah 42353, Saudi Arabia
[3] Basic and Applied Science Institute, Arab Academy for Science, Technology and Maritime Transport, Alexandria P.O. Box 1029, Egypt
[4] National Committee for Mathematics, Academy of Scientific Research and Technology, Cairo 4262104, Egypt
[5] Laboratory of Algebra, Number Theory and Nonlinear Analysis, Department of Mathematics, Faculty of Sciences, University of Monastir, Monastir 5019, Tunisia
[6] Department of Mathematics, Faculty of Sciences, University of Tabuk, Tabuk 47512, Saudi Arabia
[7] College of Sciences and Humanities in Aflaj, Prince Sattam Bin Abdulaziz University, Al Kharj 16278, Saudi Arabia
[8] Department of Mathematics, Faculty of Science, Zagazig University, Zagazig P.O. Box 44519, Egypt
* Correspondence: a.mhemdi@psau.edu.sa (A.M.); khlotfy@zu.edu.eg (K.L.)

Abstract: In this work, a novel model is presented that describes thermal diffusion processes through non-local semiconductor materials. The material under study is subjected to the influence of a strong magnetic field, which creates a Hall current. Interference between the excited electrons and the excited holes of a non-local semiconductor that had been exposed to temperature was present, and thermal conductivity depending on changes in graduated temperature were accounted for. The governing equations are written in a dimensionless form in one dimension (1D) where the thermal conductivity is taken as a function of temperature through electronic and elastic deformation (ED and ED) processes. Laplace transforms in one dimension with initial conditions were used to convert partial differential equations to arrive at exact formulas of solutions. To obtain the exact linear solutions, some boundary conditions taken on the free surface of the non-local semiconductor were used. Using numerical methods of inverse Laplace transforms, the complete solutions of the physical quantities under study were obtained. To further understand how various variables (thermal memory, variable thermal conductivity, and Hall current) affect the non-local semiconductor, numerical physical fields were simulated, and are graphically depicted, and discussed herein.

Keywords: electrons and holes; Hall current; plasma; thermal conductivity; semiconductor; photoexcitation

MSC: 74A15

check for updates

Citation: Alhashash, A.; Raddadi, M.H.; El-Bary, A.A.; Chteoui, R.; Mhemdi, A.; Lotfy, K. Thermal-Diffusive Processes of an Electron-Hole Non-Local Semiconductor Model with Variable Thermal Conductivity and Hall Current Effect. *Mathematics* **2023**, *11*, 264. https://doi.org/10.3390/math11020264

Academic Editor: Andrey Amosov

Received: 22 November 2022
Revised: 22 December 2022
Accepted: 23 December 2022
Published: 4 January 2023

Copyright: © 2023 by the authors. Licensee MDPI, Basel, Switzerland. This article is an open access article distributed under the terms and conditions of the Creative Commons Attribution (CC BY) license (https://creativecommons.org/licenses/by/4.0/).

1. Introduction

Some materials experience physical changes as a result of temperature changes. Semiconductors are among these materials because they exhibit substantial temperature-related changes in their characteristics, particularly when light beams affect their surface. The inner and outer atoms lose some electrons as a direct result of the thermal process, and these excited electrons quickly travel towards the semiconductor surface. Holes are produced as a result of the loss of electrons, and the holes also move and diffuse. This results in a change in the material's resistance because semiconductors' resistance decreases as temperature grows, allowing electric current to flow. The thermal conductivity and its characteristics must be taken into account in this situation and while examining semiconductors because they depend on the temperature gradient. Thermal conductivity is the

most significant factor that is temperature dependent. However, when semiconductor materials are exposed to a strong magnetic field, some internal physical changes also take place. These changes have a significant impact on both the transport of electrons and holes. The material deforms due to the thermal effect and magnetic field, which is caused by the vibrations and collisions of the medium's internal particles. This deformation is known as thermal (thermoelastic) deformation (TED). Furthermore, electronic deformation (ED caused by electron and hole transport processes) is brought on by the surface's absorption of light (photo) energy and the diffusion and transfer of electrons and holes that follow. According to the above-mentioned, electrons and holes are neighboring charge carriers in semiconductor materials. The photothermal (PT) theory occurs in this situation, and non-local thermoelasticity is taken into consideration. The non-local photo-thermoelasticity (PTE) theories aid in the analysis of the impact of all semiconductor medium points at the chosen local point [1].

To study how the material's physical characteristics change over time, it is essential to understand how the strong magnetic field acting on non-local semiconductor surfaces influences the Hall current. The Hall effect was found as a result of the observation that an electron concentration and position shift happens when a semiconductor is subjected to a magnetic field that is perpendicular to the direction of current flow [2]. The strength of the magnetic field surrounding the particles and the current are directly related to the potential energy between them. The Hall effect is produced as a result of the magnetic field pressure force, which moves moving-holes and electrons. The Hall effect, which is caused by the Hall current in semiconductor materials, can be used to analyze sample geometry and evaluate positive and negative conductivity in a variety of applications, including mobile chargers.

Numerous thermoelastic models were developed by Biot [3], Lord and Shulman [4], and Green and Lindsay (GL) [5] in order to derive the physical fields required by the generalized thermoelasticity theory. These models rely on the influence of temperature and elastic relaxation durations. These models have demonstrated that waves propagating within elastic materials have finite velocity, which is consistent with observations and physics theories. The overlap between the governing equations of the generalized thermoelastic theory (GTE) and the two temperature theory with several applications, has been used by various researchers to examine a variety of elastic material's physical characteristics [6–10]. It is possible to apply the photothermal (PT) approach, which describes how some media's optical and thermal properties interact, during ED and TE deformations [11].

Because light beams strike semiconductors during the processes of electron/hole diffusion, in recent years, numerous scientists have examined models that describe the interference between elastic, thermal, and light waves [12,13]. A new model that describes the interaction between holes and electrons with the propagation of thermoelastic waves in semiconductor media was studied by Sharma et al. [14]. For semiconductor sample mass diffusion and heat transport, the photoacoustic sensitivity analysis is used [15]. Modern technology uses the photothermal (PT) approach to ascertain the internal physical characteristics of semiconductors during photo-excited transport processes [16]. The relationship between the PT theory and thermoelastic theory has been researched with several applications, with consideration of the optical, thermal, and elastic properties of semiconductor materials [17–20]. When the Hall current influence of semiconductor materials is taken into account during electromagnetic field and laser pulse excitation procedures the thermal conductivity is independent of temperature. Lotfy et al. [21] and Mahdy et al. [22] have investigated numerous issues. When the link between photothermal and thermoelasticity theories was explored in the works mentioned above [23–28], the influence of interaction between holes and electrons was disregarded. The linked model of holes and electrons, on the other hand, does not consider the Hall effect or changeable thermal conductivity. When examining non-local semiconductors, most previous research has not included the impact of variable thermal conductivity on the optical characteristics in addition to the impact of the magnetic field.

The principal goal of this research is to provide a model that represents the interference between electrons and holes when the surface of a non-local semiconductor is subjected to a high magnetic field within the context of several photo-thermoelasticity models. During optically stimulated diffusion processes in the medium, the Hall current appears because of the strength of the magnetic field. This article discusses the major findings of this process during a temperature gradient and variable thermal conductivity. The model is investigated in a 1D deformation using the optical-thermal-elastic governing equations. Utilizing the Laplace transform, one can obtain analytical answers from non-dimensional primary physical fields, such as temperature, strain, mechanical stress, holes charge carrier field, and plasma intensity distributions. To achieve and determine the complete solutions in the time domain, numerical approximation is combined with some initial, boundary conditions, and the inversion of the Laplace technique. Numerous parameter effects are graphically represented.

2. Governing Equation

The induced magnetic field $h_i = (0, h_2, 0) = (0, h, 0)$ is produced in accordance with the original, extremely strong magnetic field $\vec{H} = (0, H_0, 0)$ that is present on the non-local semiconductor rod in the y-axis direction. In this case, the induced electric field $E_i = (0, 0, E)$ and the current density $J_r = (0, 0, J_3)$ are produced in the perpendicular direction of $\vec{H}$ as a result of the optical energy absorbed in the context of electronic/thermoelastic deformations diffusive processes (Figure 1) [29].

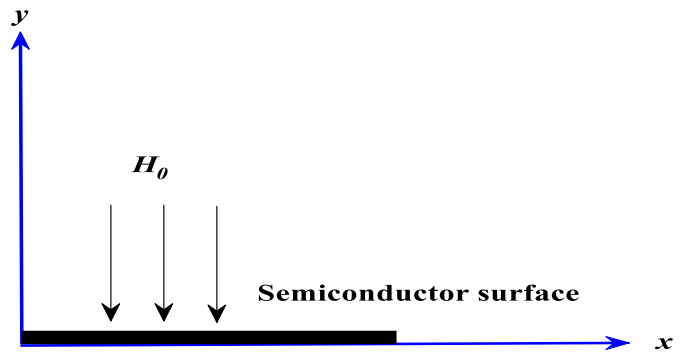


Figure 1. Schematic of the problem.

The Hall current is calculated using electromagnetic Ohm's equation in accordance with the strength pressure of the external magnetic field as shown below [30–34]:

$$\left.\begin{array}{l} J_r = \sigma_0 E_i + \mu_0 \varepsilon_{ijr} \left(u_{j,t} - \frac{\mu_0}{e n_e} J_j \right) H_r \\ F_i = \mu_0 \varepsilon_{ijr} J_j H_r, \ \ (i, j, r = (1 = x, 2 = y, 3 = z)) \end{array}\right\} \quad (1)$$

In a non-local semiconductor material, the displacement tensor is $u_j = (u_x, u_y, u_z)$, μ_0 expresses the magnetic permeability. On the other side, $u_{j,t}$ can be used to represent the displacement of the primary particle. The electrical conductivity is $\sigma_0 = n_e t_\xi e^2 / m_e$, e expresses the electron charge, m_e represents the mass of electron, n_e expresses the electrons number density, t_ξ is the collision time, and ε_{ijr} is the permutation. However, the Lorentz force F_i can be used to calculate the pressure force of a magnetic field. The induced electric field can be disregarded because of the strong magnetic field, i.e., $E = 0$. The displacement can be taken in the direction of the x-axis, according to electrons and thermoelastic deformation in one dimension (axial). However, the displacement vector takes the form:

$u_i = (u_x(x,t), 0, 0) = (u,\ 0,\ 0)$ and the strain tensor is $e = u_x = \frac{\partial u}{\partial x}$ Equation (1) can be used to determine the current density's component as follows: $J_1 = J_x = 0$, $J_2 = J_y = 0$, but the third component takes the following form (in the direction of z-axis) [20]:

$$J_3 = J_z = \frac{\sigma_0 \mu_0 H_0}{1 + m^2} \left(\frac{\partial u}{\partial t} \right) \tag{2}$$

where $m = t_\xi \omega_e$ is the Hall current parameter and $\omega_e = e\mu_0 H_0 / m_e$ represents the electron frequency.

The Lorentz's force $F_i = (F_x,\ 0,\ 0)$ can be represented as [35]:

$$F_x = \left(\frac{\sigma_0 \mu_0^2 H_0^2}{1 + m^2} \right) \frac{\partial u}{\partial t} \tag{3}$$

In addition to displacement $u(x,\ t)$, the key fields in this work include the carrier density $N(x,\ t)$ (plasma wave), temperature $T\ (x,\ t)$ (thermal wave), and the hole charge carrier field $H(x,t)$. The following governing equations in 1D can be introduced in accordance with [10] to represent the interference between thermal, elastic, and plasma (electrons and holes) waves in the absence of body forces and an internal heat source (the effect of variable thermal conductivity has been added) [10–12]:

$$\begin{aligned} (1 + \tau_\theta \tfrac{\partial}{\partial t}) \tfrac{\partial}{\partial x} \left[K \tfrac{\partial T}{\partial x} \right] + m_{nq} \tfrac{\partial^2 N}{\partial x^2} + m_{hq} \tfrac{\partial^2 H}{\partial x^2} - \rho (a_1^n \tfrac{\partial N}{\partial t} + a_1^h \tfrac{\partial H}{\partial t}) - \\ (1 + \tau_q \tfrac{\partial}{\partial t}) \left[\tfrac{K}{k} \tfrac{\partial T}{\partial t} + \rho\, T_0 \alpha_n \tfrac{\partial N}{\partial t} + \rho\, T_0 \alpha_h \tfrac{\partial H}{\partial t} + T_0 \gamma \tfrac{\partial}{\partial x} \tfrac{\partial u}{\partial t} \right] \\ = \left[\tfrac{\rho a_1^n}{t^n} N + \tfrac{\rho a_1^h}{t^h} H \right] \end{aligned} \tag{4}$$

$$\begin{aligned} m_{qn} \tfrac{\partial^2 T}{\partial x^2} + D_n \rho \tfrac{\partial^2 N}{\partial x^2} - \rho (1 - a_2^n\, T_0 \alpha_n + t^n \tfrac{\partial}{\partial t}) \tfrac{\partial N}{\partial t} - \\ a_2^n \left[\tfrac{K}{k} \tfrac{\partial T}{\partial t} + \rho\, T_0 \alpha_h \tfrac{\partial H}{\partial t} + T_0 \gamma \tfrac{\partial}{\partial x} \tfrac{\partial u}{\partial t} \right] = -\tfrac{\rho}{t_1^n} (1 + t^n \tfrac{\partial}{\partial t}) N \end{aligned} \tag{5}$$

$$\begin{aligned} m_{qh} \tfrac{\partial^2 T}{\partial x^2} + D_h \rho \tfrac{\partial^2 H}{\partial x^2} - \rho (1 - a_2^h\, T_0 \alpha_h + t^h \tfrac{\partial}{\partial t}) \tfrac{\partial H}{\partial t} - \\ a_2^h \left[\tfrac{K}{k} \tfrac{\partial T}{\partial t} + \rho\, T_0 \alpha_n \tfrac{\partial N}{\partial t} + T_0 \gamma \tfrac{\partial}{\partial t} \tfrac{\partial u}{\partial x} \right] = -\tfrac{\rho}{t_1^h} (1 + t^h \tfrac{\partial}{\partial t}) H \end{aligned} \tag{6}$$

According to Lorentz's force, the equation of motion under the influence of Hall current can be constructed as follows (the effect of a strong magnetic field has been added, in addition to the non-local parameter) [28]:

$$\begin{aligned} \rho (1 - \xi_1^2 \tfrac{\partial^2}{\partial x^2}) \tfrac{\partial^2 u}{\partial t^2} = (2\mu + \lambda) \tfrac{\partial^2 u}{\partial x^2} - \gamma (1 + \tau_\theta \tfrac{\partial}{\partial t}) \tfrac{\partial T}{\partial x} - \delta_n \tfrac{\partial N}{\partial x} - \\ \delta_h \tfrac{\partial H}{\partial x} - \left(\tfrac{\sigma_0 \mu_0^2 H_0^2}{1 + m^2} \right) \tfrac{\partial u}{\partial t} \end{aligned} \tag{7}$$

Equation (7) is differentiated relative to component x to produce:

$$\begin{aligned} \rho (1 - \xi_1^2 \tfrac{\partial^2}{\partial x^2}) \tfrac{\partial^2 e}{\partial t^2} = (2\mu + \lambda) \tfrac{\partial^2 e}{\partial x^2} - \gamma (1 + \tau_\theta \tfrac{\partial}{\partial t}) \tfrac{\partial^2 T}{\partial x^2} - \delta_n \tfrac{\partial^2 N}{\partial x^2} - \\ \delta_h \tfrac{\partial^2 H}{\partial x^2} - \left(\tfrac{\sigma_0 \mu_0^2 H_0^2}{1 + m^2} \right) \tfrac{\partial e}{\partial t} \end{aligned} \tag{8}$$

The main notations in the above equations are $a_1^n = \frac{a_{Qn}}{a_Q}$, $a_1^h = \frac{a_{Qh}}{a_Q}$, $a_2^n = \frac{a_{Qn}}{a_n}$, $a_2^h = \frac{a_{Qh}}{a_h}$ and $\frac{\rho C_e}{K} = \frac{1}{k}$ (the thermal viscosity). When the interaction between electrons and holes is taken into consideration, the constitutive equation during the 1D deformation

can be expressed as follows for the non-local semiconductor (ξ_1 is the non-local scale parameter) [28]:

$$\left.\begin{array}{l}(1-\xi_1^2\nabla^2)\sigma_{ij}=\sigma'_{ij},\\ \sigma'_{xx}=-(\gamma(1+\tau_\theta\frac{\partial}{\partial t})T+\delta_n N+\delta_h H)+(2\mu+\lambda)e=\sigma.\end{array}\right\} \tag{9}$$

The physical characteristics of non-local semiconductors are impacted by internal material deformations brought on by temperature increases. The thermal conductivity is one of the most crucial properties of a material that is impacted by the temperature differential [27,28]. Thus, it is possible to consider thermal conductivity as a linear function of temperature (temperature dependent), which can be written as:

$$K(T)=K_0(1+K_\theta T) \tag{10}$$

The parameter K_0 determines the heat conductivity in the non-local semiconductor medium when ($K_\theta=0$), and K_θ can be regarded as a small non-positive parameter [28]. The relationship between temperature and thermal conductivity, which is described as follows, is obtained using the map technique [28]:

$$\Theta=\frac{1}{K_0}\int_0^T K(\vartheta)d\vartheta \tag{11}$$

By affecting the equations by $\frac{\partial}{\partial x}$ and $\frac{\partial}{\partial t}$, yields:

$$\left.\begin{array}{l}K_0\frac{\partial\Theta}{\partial x}=K(T)\frac{\partial T}{\partial x},\\ K_0\frac{\partial\Theta}{\partial t}=K(T)\frac{\partial T}{\partial t}.\end{array}\right\} \tag{12}$$

Due to the linear characteristics of the medium, neglecting the non-linear factors results in:

$$\begin{array}{c}K_0\frac{\partial\Theta}{\partial x}=K(T)\frac{\partial T}{\partial x}\Rightarrow differentiating\ both\ sides\ by\frac{\partial}{\partial x}\Rightarrow\\ \frac{\partial}{\partial x}\left(K_0\frac{\partial\Theta}{\partial x}\right)=\frac{\partial}{\partial x}\left(K(T)\frac{\partial T}{\partial x}\right)=\\ K_0\left(\frac{\partial^2\Theta}{\partial x^2}\right)=\frac{\partial}{\partial x}\left(K_0(1+K_\theta T)\frac{\partial T}{\partial x}\right)=\\ K_0K_\theta\left\{\left(\frac{\partial T}{\partial x}\right)^2+\frac{\partial^2 T}{\partial x^2}\right\}=K_0K_\theta\frac{\partial^2 T}{\partial x^2}\end{array} \tag{13}$$

$$\frac{\partial}{\partial x}(K\frac{\partial T}{\partial x})=\frac{\partial}{\partial x}(K_0(1+K_\theta T)\frac{\partial T}{\partial x})=K_0\frac{\partial^2\Theta}{\partial x^2}+K_0K_\theta\left[\frac{\partial\Theta}{\partial x}\right]^2=K_0\frac{\partial^2\Theta}{\partial x^2} \tag{14}$$

$$\begin{array}{l}\frac{K_0}{K}\frac{\partial\Theta}{\partial x}=\frac{K_0}{K_0(1+K_\theta T)}\frac{\partial\Theta}{\partial x}=(1+K_\theta T)^{-1}\frac{\partial\Theta}{\partial x}=(1-K_\theta T+(K_\theta T)^2-\ldots)\frac{\partial\Theta}{\partial x}=\\ \frac{\partial\Theta}{\partial x}-K_\theta T\frac{\partial\Theta}{\partial x}+(K_\theta T)^2\frac{\partial\Theta}{\partial x}-\ldots=\frac{\partial\Theta}{\partial x}\end{array} \tag{15}$$

Equations (10)–(15) of the fundamental Equations (4)–(7) after applying the above map transformations result in:

$$\begin{array}{c}(1+\tau_\theta\frac{\partial}{\partial t})\frac{\partial}{\partial x}\left[K_0\frac{\partial\Theta}{\partial x}\right]+m_{nq}\frac{\partial^2 N}{\partial x^2}+m_{hq}\frac{\partial^2 H}{\partial x^2}-\rho(a_1^n\frac{\partial N}{\partial t}+a_1^h\frac{\partial H}{\partial t})-\\ (1+\tau_q\frac{\partial}{\partial t})\left[\frac{K_0}{k}\frac{\partial\Theta}{\partial t}+\rho\,T_0\alpha_n\frac{\partial N}{\partial t}+\rho\,T_0\alpha_h\frac{\partial H}{\partial t}+T_0\gamma\frac{\partial}{\partial x}\frac{\partial u}{\partial t}\right]\\ =\left[\frac{\rho a_1^n}{t^n}N+\frac{\rho a_1^h}{t^h}H\right]\end{array} \tag{16}$$

$$\frac{m_{qn}}{K_\theta}\frac{\partial^2\Theta}{\partial x^2} + D_n\rho\frac{\partial^2 N}{\partial x^2} - \rho(1 - a_2^n\, T_0\alpha_n + t^n\frac{\partial}{\partial t})\frac{\partial N}{\partial t} - a_2^n\left[\frac{K_0}{k}\frac{\partial\Theta}{\partial t} + \rho\, T_0\alpha_h\frac{\partial H}{\partial t} + T_0\gamma\frac{\partial}{\partial x}\frac{\partial u}{\partial t}\right] = -\frac{\rho}{t_1^n}(1 + t^n\frac{\partial}{\partial t})N \tag{17}$$

$$\frac{m_{qh}}{K_\theta}\frac{\partial^2\Theta}{\partial x^2} + D_h\rho\frac{\partial^2 H}{\partial x^2} - \rho(1 - a_2^h\, T_0\alpha_h + t^h\frac{\partial}{\partial t})\frac{\partial H}{\partial t} - a_2^h\left[\frac{K_0}{k}\frac{\partial\Theta}{\partial t} + \rho\, T_0\alpha_n\frac{\partial N}{\partial t} + T_0\gamma\frac{\partial}{\partial t}\frac{\partial u}{\partial x}\right] = -\frac{\rho}{t_1^h}(1 + t^h\frac{\partial}{\partial t})H \tag{18}$$

$$\rho\,(1 - \xi_1^2\frac{\partial^2}{\partial x^2})\,\frac{\partial^2 e}{\partial t^2} = (2\mu + \lambda)\frac{\partial^2 e}{\partial x^2} - \gamma(1 + \tau_\theta\frac{\partial}{\partial t})\frac{\partial^2\Theta}{\partial x^2} - \delta_n\frac{\partial^2 N}{\partial x^2} - \delta_h\frac{\partial^2 H}{\partial x^2} - \left(\frac{\sigma_0\mu_0^2 H_0^2}{1+m^2}\right)\frac{\partial e}{\partial t} \tag{19}$$

The following dimensionless quantities can be introduced as follows for greater appropriateness:

$$\left.\begin{array}{l}(x', u',\, \xi'_1) = \frac{\omega^*(x,u,\xi_1)}{C_T},\ (t', \tau'_q, \tau'_\theta, t^{n'}, t^{h'}, t_1^{n'}, t_1^{h'}) = \omega^*(t,\, \tau_q, \tau_\theta, t^n, t^h, t_1^n, t_1^h),\\ \beta^2 = \frac{C_T^2}{C_L^2},\ k = \frac{K}{\rho C_e},\ \sigma'_{ij} = \frac{\sigma_{ij}}{2\mu+\lambda},\ N' = \frac{\delta_n(N)}{2\mu+\lambda},\ C_T^2 = \frac{2\mu+\lambda}{\rho},\ C_L^2 = \frac{\mu}{\rho},\\ \omega^* = \frac{C_e(\lambda+2\mu)}{K},\ (\overline{\delta}_n, \overline{\delta}_h) = \frac{(\delta_n n_0, \delta_h h_0)}{\gamma T_0},\ \Theta' = \frac{\gamma(\Theta)}{2\mu+\lambda}, H' = \frac{\delta_n(H)}{2\mu+\lambda}.\end{array}\right\} \tag{20}$$

Equation (20), which ignores the dashes in favor of the primary Equations (8) and (16)–(19) results in:

$$\left\{(1 + \tau_\theta\frac{\partial}{\partial t})\frac{\partial^2}{\partial x^2} - (1 + \tau_q\frac{\partial}{\partial t})\frac{\partial}{\partial t}\right\}\Theta + \left\{\alpha_1\frac{\partial^2}{\partial x^2} - \alpha_2(1 + \tau_q\frac{\partial}{\partial t}) - \alpha_3\frac{\partial}{\partial t} - \alpha_4\right\}N + \left\{\alpha_5\frac{\partial^2}{\partial x^2} - (1 + \tau_\alpha\frac{\partial}{\partial t})\alpha_6 - \alpha_7\right\}H - (1 + \tau_q\frac{\partial}{\partial t})\varepsilon_1\frac{\partial e}{\partial t} = 0 \tag{21}$$

$$\left\{\frac{\partial^2}{\partial x^2} - \alpha_8\frac{\partial}{\partial t}\right\}\Theta + \left\{\alpha_9\frac{\partial^2}{\partial x^2} - (\alpha_{10} + t^n\frac{\partial}{\partial t})\alpha_{11} + (1 + t^n\frac{\partial}{\partial t})\frac{\alpha_{11}}{t^n}\right\}N - \alpha_{12}\frac{\partial H}{\partial t} - \alpha_{13}\frac{\partial e}{\partial x} = 0 \tag{22}$$

$$\left\{\frac{\partial^2}{\partial x^2} - \alpha_{18}\frac{\partial}{\partial t}\right\}\Theta + \left\{\alpha_{14}\frac{\partial^2}{\partial x^2} - (\alpha_{15} + t^h\frac{\partial}{\partial t})\alpha_{16}\frac{\partial}{\partial t} + (1 + t^h\frac{\partial}{\partial t})\alpha_{17}\right\}H - \alpha_{19}\frac{\partial N}{\partial t} - \alpha_{20}\frac{\partial e}{\partial t} = 0 \tag{23}$$

$$\left(\frac{\partial^2}{\partial x^2} - \left[(1 - \xi_1^2\frac{\partial^2}{\partial x^2})\frac{\partial^2}{\partial t^2} + \left(\frac{M}{1+m^2}\right)\frac{\partial}{\partial t}\right]\right)e - (1 + \tau_\theta\frac{\partial}{\partial t})\frac{\partial^2\Theta}{\partial x^2} - \frac{\partial^2 N}{\partial x^2} - \frac{\partial^2 H}{\partial x^2} \tag{24}$$

$$\sigma = \left(e - (\,(1 + \tau_\theta\frac{\partial}{\partial t})\Theta + N)\right) - H \tag{25}$$

In this case, $M = \frac{\sigma_0 t^* \mu_0^2 H_0^2}{\rho}$, which stands for the Hartmann number, can be used to determine the magnetic pressure number's strength. Other coefficients include:

$$\alpha_1 = \frac{m_{nq}\alpha_t}{d_n K_0}, \alpha_2 = \frac{T_0\alpha_n}{C_e}, \alpha_3 = \frac{a_1^n}{C_e}, \alpha_4 = \frac{a_1^n\gamma}{C_e\tau^n(2\mu+\lambda)}, \alpha_5 = \frac{\gamma m_{hq}\, h_0}{(2\mu+\lambda)K_0}, \alpha_6 = \frac{T_0\,\alpha_h\, K_0\, h_0}{C_e},$$

$$\alpha_7 = \frac{a_1^h\gamma\omega^*}{t^h K_0}, \alpha_8 = \frac{a_2^n K_1}{m_{qn}}, \alpha_9 = \frac{D_n\rho\alpha_t}{m_{qn}\, d_n}, \alpha_{10} = 1 - a_2^n T_0\alpha_n, \alpha_{11} = \frac{\alpha_t K_0}{m_{qn}\, d_n C_e}, \alpha_{12} = \frac{a_2^n\gamma h_0\alpha_h\omega^*}{m_{qn}},$$

$$\alpha_{13} = \frac{a_2^n\gamma^2 T_0\omega^*}{\rho\, m_{qn}}, \alpha_{14} = \frac{D_n h_0\gamma}{C_T^2\, m_{qh}}, \alpha_{15} = 1 - a_2^h T_0\alpha_n, \alpha_{16} = \frac{\gamma h_0\omega^*}{m_{qh}}, \alpha_{17} = \frac{\gamma h_0\omega^*}{m_{qh}\tau_1^h}, \alpha_{18} = a_2^h\frac{K_1}{m_{qh}},$$

$$\alpha_{19} = \frac{a_2^h\gamma T_0\alpha_n(2\mu+\lambda)\omega^*}{m_{qh}\delta_n}, \alpha_{20} = \frac{a_2^h\gamma^2 T_0\,\omega^*}{m_{qh}\rho}, \varepsilon_1 = \frac{T_0\gamma^2\omega^*}{\rho K_0}.$$

When the medium is homogenous at time $t = 0.0$, the following initial conditions are posited and can be expressed as follows:

$$\begin{aligned} e(x,\,t)|_{t=0} &= \left.\frac{\partial e(x,t)}{\partial t}\right|_{t=0} = 0,\; T(x,t)|_{t=0} = \left.\frac{\partial T(x,t)}{\partial t}\right|_{t=0} = 0, \\ H(x,t)|_{t=0} &= \left.\frac{\partial H(x,t)}{\partial t}\right|_{t=0} = 0,\; N(x,t)|_{t=0} = \left.\frac{\partial N(x,t)}{\partial t}\right|_{t=0} = 0 \end{aligned} \tag{26}$$

3. Analytical Solution Procedure

It is possible to use the Laplace transform approach with parameter s for the governing equations, which can be written as follows for function $\cap(x,\,t)$ [30]:

$$L(\cap(x,\,t)) = \overline{\cap}(x,\,s) = \int_0^\infty \cap(x,\,t)\mathrm{e}^{-st}\,d\,t \tag{27}$$

Utilizing the initial conditions for the principal system (21)–(25) and the Laplace transform equation (27) results in:

$$\left(q_1\,D^2 - q_2\right)\overline{\Theta} + \left(\alpha_1 D^2 - q_3\right)\overline{N} + \left(\alpha_5 D^2 - q_4\right)\overline{H} - q_5\bar{e} = 0 \tag{28}$$

$$\left(D^2 - q_7\right)\overline{\Theta} + \left(\alpha_9 D^2 - q_6\right)\overline{N} - q_8\overline{H} - q_9\bar{e} = 0 \tag{29}$$

$$\left(D^2 - q_{10}\right)\overline{\Theta} + \left(\alpha_{14} D^2 - q_{11}\right)\overline{H} - q_{12}\overline{N} - q_{13}\bar{e} = 0 \tag{30}$$

$$\left(D^2 - \Upsilon\right)\bar{e} - q_{14}D^2\overline{\Theta} - \alpha_{21}D^2\overline{N} - \alpha_{21}D^2\overline{H} = 0 \tag{31}$$

$$\overline{\sigma} = \left(\bar{e} - \left((1 + s\tau_\theta)\overline{\Theta} + \overline{N}\right)\right) - \overline{H} \tag{32}$$

where,
$D = \frac{d}{dx}$, $q_1 = (1 + \tau_\theta\frac{\partial}{\partial t})$, $\Re_H = s^2 + s\frac{M}{1+m^2}$, $\Upsilon = \frac{\Re_H}{1+\zeta_1^2 s^2}$, $q_2 = (1 + \tau_q\frac{\partial}{\partial t})\,s$, $q_4 = (1 + \tau_q\frac{\partial}{\partial t})\alpha_6 + \alpha_7$, $q_{14} = \frac{1+\tau_\theta s}{1+\zeta_1^2 s^2}$, $q_3 = \left(\alpha_2(1 + \tau_q\frac{\partial}{\partial t}) + \alpha_3\frac{\partial}{\partial t} + \alpha_4\right)$, $q_6 = (\alpha_{10} + t^n s)\alpha_{11} - (1 + t^n s)\frac{\alpha_{11}}{t^n}$, $\alpha_{21} = \frac{1}{1+\zeta_1^2 s^2}$, $q_{14} = 1 + \tau_\theta s$, $q_9 = \alpha_{13}\,s$, $q_{10} = \alpha_{18}s$, $q_5 = (1 + \tau_q\,s)\varepsilon_1\,s$, $q_7 = \alpha_8\,s$, $q_8 = \alpha_{12}s$, $q_{12} = \alpha_{19}s$, $q_{13} = \alpha_{20}s$, $q_{11} = (\alpha_{15} + t^h s)\alpha_{16}s - (1 + t^h s)\alpha_{17}$.

Using the elimination approach in terms of $\overline{\Theta}$, $\bar{e}$, $\overline{N}$ and $\overline{H}$, the resultant system of the governing Equations (28)–(31) is solved to provide the equation shown below:

$$(D^8 - \prod_1 D^6 + \prod_2 D^4 - \prod_3 D^2 + \prod_4)\{\overline{H}, \overline{N}, \overline{\Theta}, \bar{e}\}(x,s) = 0 \tag{33}$$

Equation (33) can be factored as follows (the main coefficients of equation (33) can be obtained in the Appendix A):

$$\left(D^2 - m_1^2\right)\left(D^2 - m_2^2\right)\left(D^2 - m_3^2\right)\left(D^2 - m_4^2\right)\{\,\overline{\Theta},\,\bar{e},\,\overline{N},\,\overline{H}\}(x,s) = 0 \tag{34}$$

where m_1^2, m_2^2, m_3^2, and m_4^2 are the real-roots of the above characteristic (34) at $x \to \infty$. The following format can be used to express the linear solutions for physical fields in the Laplace domain:

$$\overline{\Theta}(x,\,s) = \sum_{i=1}^{4} \mathrm{B}_i(s)\,e^{-m_i x} \tag{35}$$

$$\overline{N}(x,\, s) = \sum_{i=1}^{4} \mathrm{B'}_i(s)\, e^{-m_i x} = \sum_{i=1}^{4} H_{1i} \mathrm{B}_i(s)\, e^{-m_i x} \tag{36}$$

$$\overline{e}(x,s) = \sum_{i=1}^{4} \mathrm{B}_i{}''(s)\ \exp(-m_i x) = \sum_{i=1}^{4} H_{2i}\, \mathrm{B}_i(s)\ \exp(-m_i x) \tag{37}$$

$$\overline{H}\,(x,s) = \sum_{i=1}^{4} \mathrm{B'''}_i(s)\ \exp(-m_i x) = \sum_{i=1}^{4} H_{3i}\, \mathrm{B}_i(s)\ \exp(-m_i x) \tag{38}$$

$$\overline{\sigma}\,(x,s) = \sum_{i=1}^{4} \left(\mathrm{B}_i^{'''\prime}(s)\right) \exp(-m_i x) = \sum_{i=1}^{4} \left(H_{4i}\, \mathrm{B}_i(s)\right)\ \exp(-m_i x) \tag{39}$$

where, the principal coefficients of the above equations are:

$$\left.\begin{aligned} H_{1i} &= -\tfrac{\alpha_{14} m_i^6 + c_7 m_i^4 + c_8 m_i^2 + c_9}{\alpha_9 \alpha_{14} m_i^6 + c_4 m_i^4 + c_5 m_i^2 + c_6}, \\ H_{2i} &= \tfrac{c_{10} m_i^6 + c_{11} m_i^4 + c_{12} m_i^2}{\alpha_9 \alpha_{14} m_i^6 + c_4 m_i^4 + c_5 m_i^2 + c_6}, \\ H_{3i} &= -\tfrac{\alpha_9 m_i^6 + c_1 m_i^4 + c_2 m_i^2 + c_3}{\alpha_9 \alpha_{14} m_i^6 + c_4 m_i^4 + c_5 m_i^2 + c_6}, \\ H_{4i} &= (H_{2i} - ((1 + s\tau_\theta) H_{1i} + 1) - H_{3i}). \end{aligned}\right\} \tag{40}$$

4. Applications (Thermal Ramp Type)

To establish the value of the undetermined parameters, the thermal ramp type, mechanical, and plasma conditions are applied to the free surface of the medium at $x = 0$. However, the following format might be used to express the conditions [31].

(I) The ramp type heating is where the thermal boundary is taken from $x = 0$ with thermal load $\widetilde{T}$ as [27,28]:

$$\overline{\Theta}(0,t) = \begin{cases} 0 & t \le 0 \\ \frac{t}{t_0} & 0 < t \le t_0 \\ 1 & t > t_0 \end{cases} \tag{41}$$

in this case,

$$\sum_{n=1}^{4} \mathrm{B}_i(s) = \widetilde{T}(\xi) \frac{\left(1 - e^{-st_0}\right)}{t_0 s^2} \tag{42}$$

(II) The mechanical condition at the free surface $x = 0$ can be obtained with loaded force P as:

$$\left.\begin{aligned} \overline{\sigma}(0,s) &= \overline{P} \\ \sum_{i=1}^{4} H_{4i}\, \mathrm{B}_i(s) &= \overline{P} \end{aligned}\right\} \tag{43}$$

(III) When the carrier density spreads throughout the recombination processes and the medium is exhausted with mass and heat transmission, the plasma condition can be applied at the surface $x = 0$. However, this condition can be expressed as follows under the influence of the Laplace transform:

$$\left.\begin{aligned} \overline{N}(0,\, s) &= \tfrac{\widetilde{s}\hat{\boldsymbol{\lambda}} n_0}{D_e} \\ \sum_{i=1}^{4} H_{1i} \mathrm{B}_i(s) &= \tfrac{\hat{\boldsymbol{\lambda}} \widetilde{s} n_0}{D_e} \end{aligned}\right\} \tag{44}$$

(IV) During the optical-excitation processes at the surface $x = 0$, the recombination diffusion for the holes charge field also occurs, which, in the equilibrium situation, can be expressed under the Laplace transform as follows:

$$\left.\begin{array}{l} \overline{H}(0,s) = h_0 \\ \sum\limits_{i=1}^{4} H_{3i}\,\mathrm{B}_i(s) = h_0 \end{array}\right\} \tag{45}$$

where $\mathfrak{\lambda}$ is a chosen (positive) parameter.

5. Inversion Processes of the Laplace Transforms

To obtain the complete solutions in the time domain, the Riemann-sum approximation is numerically applied, and the inversion of the Laplace transform is employed for the key fields. According to its integral form, the Laplace transform inversion of a function $\mathbb{Z}(x,\, s)$ can be expressed as follows [31]:

$$\mathbb{Z}(x,\, t') = L^{-1}\{\overline{\mathbb{Z}}(x,\, s)\} = \frac{1}{2\pi i}\int_{n-i\infty}^{n+i\infty} \exp(st')\overline{\mathbb{Z}}(x,\, s)ds \tag{46}$$

Equation (50) can, however, be rewritten as follows:

$$\mathbb{Z}(x,\, t') = \frac{\exp(nt')}{2\pi}\int_{\infty}^{\infty} \exp(i\beta t)\overline{\mathbb{Z}}(x,\, n+i\beta)d\beta \tag{47}$$

When applied to the interval $[0,\, 2t']$ for the function $\mathbb{Z}(x,\, s)$, the Fourier series expansion results in:

$$\mathbb{Z}(x,\, t') = \frac{e^{nt'}}{t'}\left[\frac{1}{2}\overline{\mathbb{Z}}(x,\, n) + Re\sum_{k=1}^{N}\overline{\mathbb{Z}}(x, n+\frac{ik\pi}{t'})(-1)^n\right] \tag{48}$$

where $i = \sqrt{-1}$, $n \in R$ (real numbers), N chosen freely, and the symbol Re expresses the real part and the notation $nt' \approx 4.7$ approximately [31].

On the other hand, the temperature distribution can be determined from the temperature plotted using the following relation, which assumes linearity:

$$\Theta = \frac{1}{K_0}\int_0^T K_0(1+K_\theta T)dT = T + \frac{K_\theta}{2}T^2 = \frac{K_\theta}{2}(T+\frac{1}{K_\theta})^2 - \frac{1}{2K_\theta} \tag{49}$$

The temperature distribution in this instance can be calculated in terms of Θ as follows:

$$T = \frac{1}{K_\theta}\left[\sqrt{1+2K_\theta\Theta} - 1\right] \Leftrightarrow \overline{T} = \frac{1}{K_\theta}\left[\sqrt{1+2K_\theta\overline{\Theta}} - 1\right] \tag{50}$$

6. Validation

6.1. The Non-Local Photo-Thermoelasticity Models

During various comparisons with earlier investigations, the whole solutions are validated. The various thermal and elastic relaxation durations can be used to categorize the photo-thermoelasticity hypotheses. The following models fit within these categories [3–5]:

(1) When $0 \le \tau_\theta < \tau_q$, expresses the dual phase lag DPL model.
(2) When $\tau_\theta = 0$, $0 < \tau_q$, expresses the Lord and Ṣhulman (LS) model.
(3) When $\tau_\theta = \tau_q = 0.0$, expresses the coupled thermoelasticity (CT) model.

6.2. Effect of Strong Magnetic Field

When $H_0 = 0$, the photo-thermoelasticity theory with holes and electrons interaction is obtained with variable thermal conductivity while disregarding the Hall current impact and Hartmann number [32].

6.3. The Non-Local Semiconductor Medium

When the effects of the non-local scale parameter are disregarded ($\xi_1 = 0.0$), the photo-thermoelasticity theories are obtained under the influence of the Hall current and variable thermal conductivity when the electron/hole interaction is considered.

6.4. The Non-Local Magneto-Photo-Thermoelasticity Theory with Variable Thermal Conductivity

The generalized photo-thermoelasticity theory under the influence of a strong magnetic field with variable thermal conductivity is examined when the holes carrier charge field (holes carrier density) is vanishing, that is, $H = 0$. However, only these equations remain from the governing equations [33,34]:

$$\left.\begin{aligned}\left\{(1+\tau_\theta\tfrac{\partial}{\partial t})\tfrac{\partial^2}{\partial x^2} - (1+\tau_q\tfrac{\partial}{\partial t})\tfrac{\partial}{\partial t}\right\}\Theta + \left\{\alpha_1\tfrac{\partial^2}{\partial x^2} - \alpha_2(1+\tau_q\tfrac{\partial}{\partial t}) - \alpha_3\tfrac{\partial}{\partial t} - \alpha_4\right\}N \\ = (1+\tau_q\tfrac{\partial}{\partial t})\varepsilon_1\tfrac{\partial e}{\partial t}\end{aligned}\right\} \quad (51)$$

$$\left\{\frac{\partial^2}{\partial x^2} - \alpha_8\frac{\partial}{\partial t}\right\}\Theta + \left\{\alpha_9\frac{\partial^2}{\partial x^2} - (\alpha_{10}+t^n\frac{\partial}{\partial t})\alpha_{11} + (1+t^n\frac{\partial}{\partial t})\frac{\alpha_{11}}{t^n}\right\}N = \alpha_{13}\frac{\partial e}{\partial x} \quad (52)$$

$$\left(\frac{\partial^2}{\partial x^2} - \left[(1-\xi_1^2\frac{\partial^2}{\partial x^2})\frac{\partial^2}{\partial t^2} + \left(\frac{M}{1+m^2}\right)\frac{\partial}{\partial t}\right]\right)e - (1+\tau_\theta\frac{\partial}{\partial t})\frac{\partial^2\Theta}{\partial x^2} - \frac{\partial^2 N}{\partial x^2} \quad (53)$$

6.5. The Impact of Thermal Conductivity

The problem is examined within the framework of the generalized non-local photo-thermoelasticity theory with Hall current influence when the thermal conductivity of the medium is independent of temperature, as it is in this instance for $K = K_0$ and $K_\theta = 0$. The system of equations in this instance is simplified as follows [36]:

$$\left.\begin{aligned}\left((1+\tau_\theta\tfrac{\partial}{\partial t})\tfrac{\partial^2}{\partial x^2} - (1+\tau_q\tfrac{\partial}{\partial t})\tfrac{\partial}{\partial t}\right)T + \left(\alpha_1\tfrac{\partial^2}{\partial x^2} - \alpha_2(1+\tau_q\tfrac{\partial}{\partial t}) - \alpha_3\tfrac{\partial}{\partial t} - \alpha_4\right)N + \\ \left(\alpha_5\tfrac{\partial^2}{\partial x^2} - (1+\tau_\alpha\tfrac{\partial}{\partial t})\alpha_6 - \alpha_7\right)H = (1+\tau_q\tfrac{\partial}{\partial t})\varepsilon_1\tfrac{\partial e}{\partial t}\end{aligned}\right\} \quad (54)$$

$$\left.\begin{aligned}\left\{\tfrac{\partial^2}{\partial x^2} - \alpha_8\tfrac{\partial}{\partial t}\right\}T + \left\{\alpha_9\tfrac{\partial^2}{\partial x^2} - (\alpha_{10}+t^n\tfrac{\partial}{\partial t})\alpha_{11} + (1+t^n\tfrac{\partial}{\partial t})\tfrac{\alpha_{11}}{t^n}\right\}N - \\ \alpha_{12}\tfrac{\partial H}{\partial t} - \alpha_{13}\tfrac{\partial e}{\partial t} = 0\end{aligned}\right\} \quad (55)$$

$$\left.\begin{aligned}\left\{\tfrac{\partial^2}{\partial x^2} - \alpha_{18}\tfrac{\partial}{\partial t}\right\}T + \left\{\alpha_{14}\tfrac{\partial^2}{\partial x^2} - (\alpha_{15}+t^h\tfrac{\partial}{\partial t})\alpha_{16}\tfrac{\partial}{\partial t} + (1+t^h\tfrac{\partial}{\partial t})\alpha_{17}\right\}H - \\ \alpha_{19}\tfrac{\partial N}{\partial t} - \alpha_{20}\tfrac{\partial e}{\partial t} = 0\end{aligned}\right\} \quad (56)$$

$$\left(\frac{\partial^2}{\partial x^2} - \left[(1-\xi_1^2\frac{\partial^2}{\partial x^2})\frac{\partial^2}{\partial t^2} + \left(\frac{M}{1+m^2}\right)\frac{\partial}{\partial t}\right]\right)e - (1+\tau_\theta\frac{\partial}{\partial t})\frac{\partial^2 T}{\partial x^2} - \frac{\partial^2 N}{\partial x^2} - \frac{\partial^2 H}{\partial x^2} = 0 \quad (57)$$

7. Numerical Results and Discussions

This section investigates wave propagation in the semiconductor medium by numerically simulating (as a result of using Matlab 2020, a rapid Fourier transform-based numerical inversion of the Laplace transform (NILT) approach is used [36]) the primary physical fields (temperature, stress, holes charge carrier field, and plasma (carrier density) distributions). For the simulation, silicon (Si) material's physical constants are employed.

The following parameters are utilized in SI units and are listed in Table 1 in order to carry out the numerical simulations and discussion [37–41]:

Table 1. The physical input parameters of Si medium in SI units.

Unit	Symbol	Value	Unit	Symbol	Value
Nm^{-2}	λ μ	6.4×10^{10} 6.5×10^{10}	m^3	d_n	-9×10^{-31}
$kg{\cdot}m^{-3}$	ρ	2330	sec (s)	τ_0	0.00005
K	T_0	800	$V{\cdot}K^{-1}$	m_{qn}	1.4×10^{-5}
sec (s)	τ	5×10^{-5}	$V{\cdot}K^{-1}$	m_{nq}	1.4×10^{-5}
K^{-1}	α_t	4.14×10^{-6}	$V{\cdot}K^{-1}$	m_{qh}	-0.004×10^{-6}
$W{\cdot}m^{-1}{\cdot}K^{-1}$	k	150	$V{\cdot}K^{-1}$	m_{hq}	-0.004×10^{-6}
$J{\cdot}kg^{-1}{\cdot}K^{-1}$	C_e	695	$m^2{\cdot}s^{-1}$	D_n	0.35×10^{-2}
$Col^2{\cdot}Cl^{-1}{\cdot}cm^{-1}{\cdot}s^{-1}$	σ_0	9.36×10^5	$m^2{\cdot}s^{-1}$	D_h	0.125×10^{-2}
$m{\cdot}s^{-1}$	$\widetilde{s}$	2	m^{-3}	$\widetilde{n}_0$	10^{20}
	$\mathfrak{\lambda}$	2	$m^2{\cdot}s^{-1}$	α_n	1×10^{-2}
m^{-3}	h_0	10^{20}	$m^2{\cdot}s^{-1}$	α_h	5×10^{-3}
$m^2{\cdot}s^{-1}$	D_e	2.5×10^{-3}	$H{\cdot}m^{-1}$	μ_0	$4\pi \times 10^{-7}$

7.1. The Photo-Thermoelasticity Models

The variations of the important physical fields (thermal waves (thermal temperature), normal stress (mechanical waves), holes charge carrier field, and plasma waves (carrier density)) against the axial distance are numerically calculated and graphed in three groups based on the input parameters of silicon suggested above (Figures 2–5). Dimensionless quantities are used in all calculations with a small time $t = 0.0001$ in the non-local case when $\xi_1 = 0.50$ [42,43]. Figure 2 (first group) displays the linked photo-thermoelasticity models for the various relaxation times when the Hall current influence is present and the non-local semiconductor medium is temperature dependent (at $K_\theta = -0.4$) [34,36,37]. The first subfigure shows how dimensionless thermal waves that begin at the free surface at zero point and meet the thermal boundary condition (ramp type heating) propagate against distance. Due to the absorbed optical energy and Hall current action (strong magnetic field), the thermal waves grow dramatically as they go closer to the outer surface until they reach their peak maximum point. The spread of the thermal waves decreases exponentially as the influence of the absorbed light energy and the strong magnetic field inside the material decreases, reaching its minimal value and approaching the zero line before dissipating with increasing distance. The second sub-figure displays the differences in mechanical waves' (normal stress) distribution versus distance using photo-thermoelasticity models, the distribution of the mechanical waves beginning at the surface, and the negative value that satisfies the mechanical load condition. The distribution initially decreases within the material for a very short distance before it slowly over time rises away from the surface until it approaches the maximum value before it converges to the zero line as a result of the effects of the absorbed optical energy and the effect of the strong magnetic field (state of equilibrium). The hole carrier charge distributions begin with a positive value at the surface and quickly increase in accordance with the recombination processes to reach the maximum value due to the Hall current impact and thermal effect of the optical energy (the third subfigure). The hole charge carrier distribution starts to steadily decrease away from the surface in the shape of an exponential wave until it reaches the region of stability close to the zero line. According to several photo-thermoelasticity models, the carrier density (plasma waves) against axial distance is depicted in the fourth subfigure. The plasma waves begin with a positive value and develop gradually until they reach their maximum values

during the recombination processes, absorbed optical energy, and a strong magnetic field on the outer surface. On the other hand, as the plasma wave approaches the zero line, it gradually starts to decrease, fleeing from the surface and propagating as an exponential wave. It is evident from Figure 2 that the different relaxation times lead to different wave propagation behavior for the fundamental quantities under study. Taking into account the increase in relaxation times, the DPL model is more realistic compared to the other models, is physically acceptable, and is consistent with the experimental results implemented by Xiao et al. [44]. The thermal wave and plasma wave behavior are compatible with those of the experiments specified in the subfigures of temperature and carrier density distribution [45].

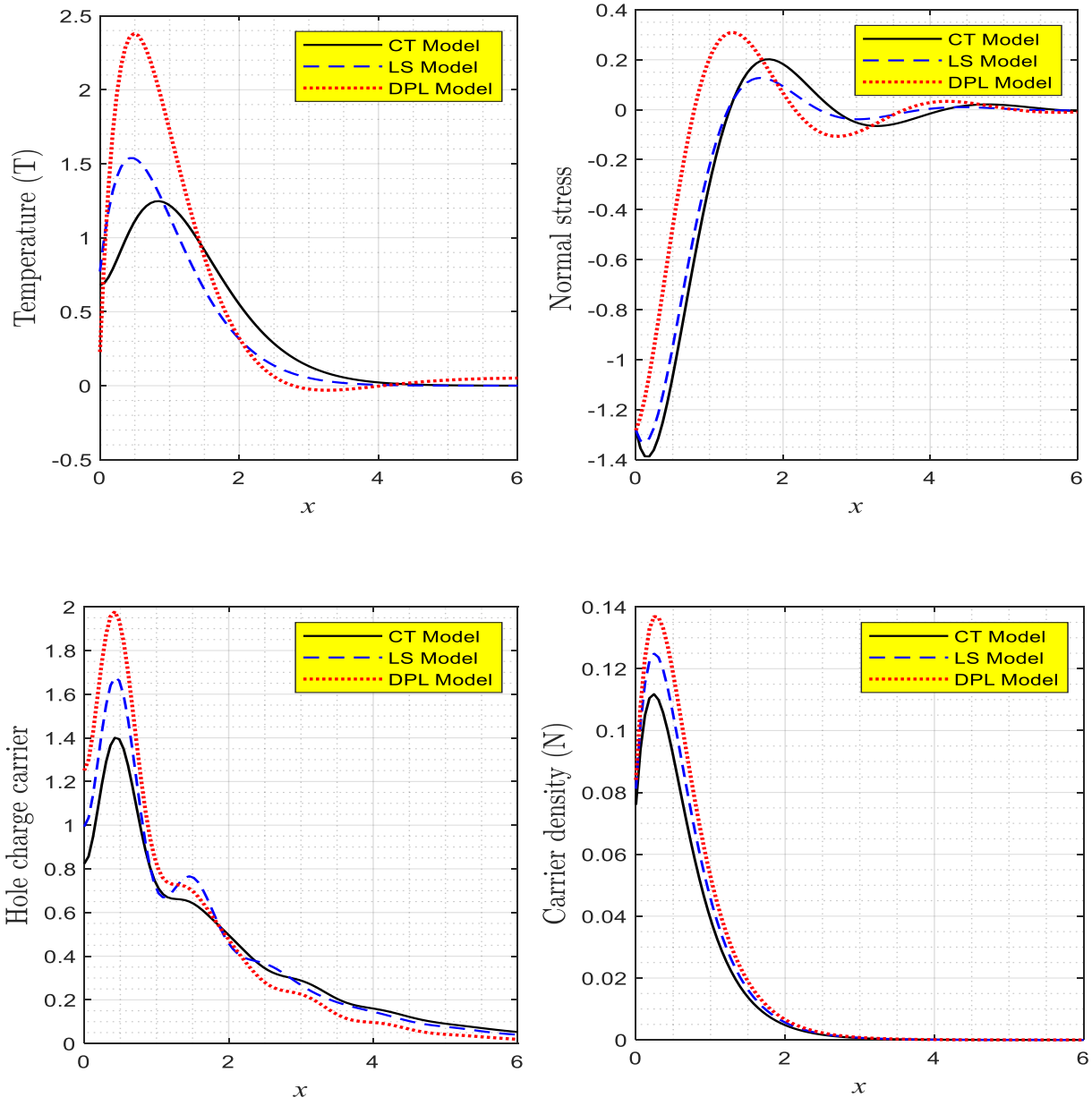


Figure 2. According to photo-thermoelasticity models with varying thermal conductivity under the influence of Hall current, the principal non-local physical distributions change with distance.

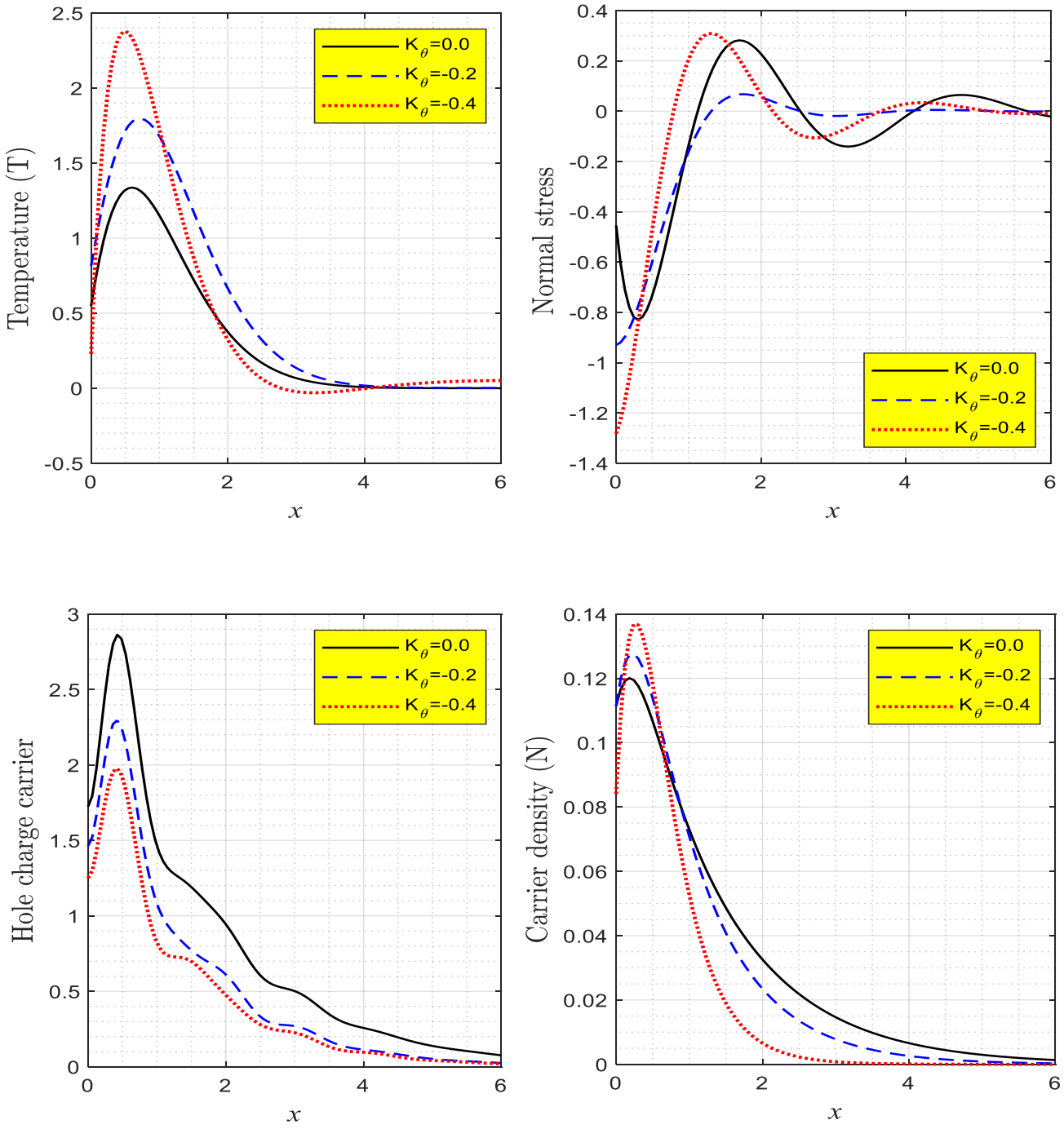


Figure 3. According to the DPL model, the three examples of variable thermal conductivity show a variance in the non-local physical field distributions as a function of axial distance.

7.2. The Effect of Variable Thermal Conductivity

When the thermal conductivity of the non-local semiconductor medium relies on temperature, the principal physical fields' variations versus axial distance are shown in the second group (Figure 3). According to the DPL model, the computations are performed when $t = 0.0001$ under the effect of Hall current in the non-local case when $\xi_1 = 0.50$. Three cases that depend on the value of K_θ (in the range $-10^{-3} \leq K_\theta \leq 10^{-2}$ for the non-local semiconductor medium) are explored when $K(T) = K_0(1 + K_\theta T)$ [37]. The first case is when $K_\theta = 0$, or when $K = K_0$, refers to the medium in a temperature-independent situation [39–41]. However, the other two cases $K_\theta = -0.2$ and $K_\theta = -0.4$ describe the

case in which the thermal conductivity of the medium is temperature-dependent. The amplitudes of the thermal wave, mechanical wave, hole charge carrier field, and plasma wave all rise with rising values of K_θ, according to various values of K_θ.

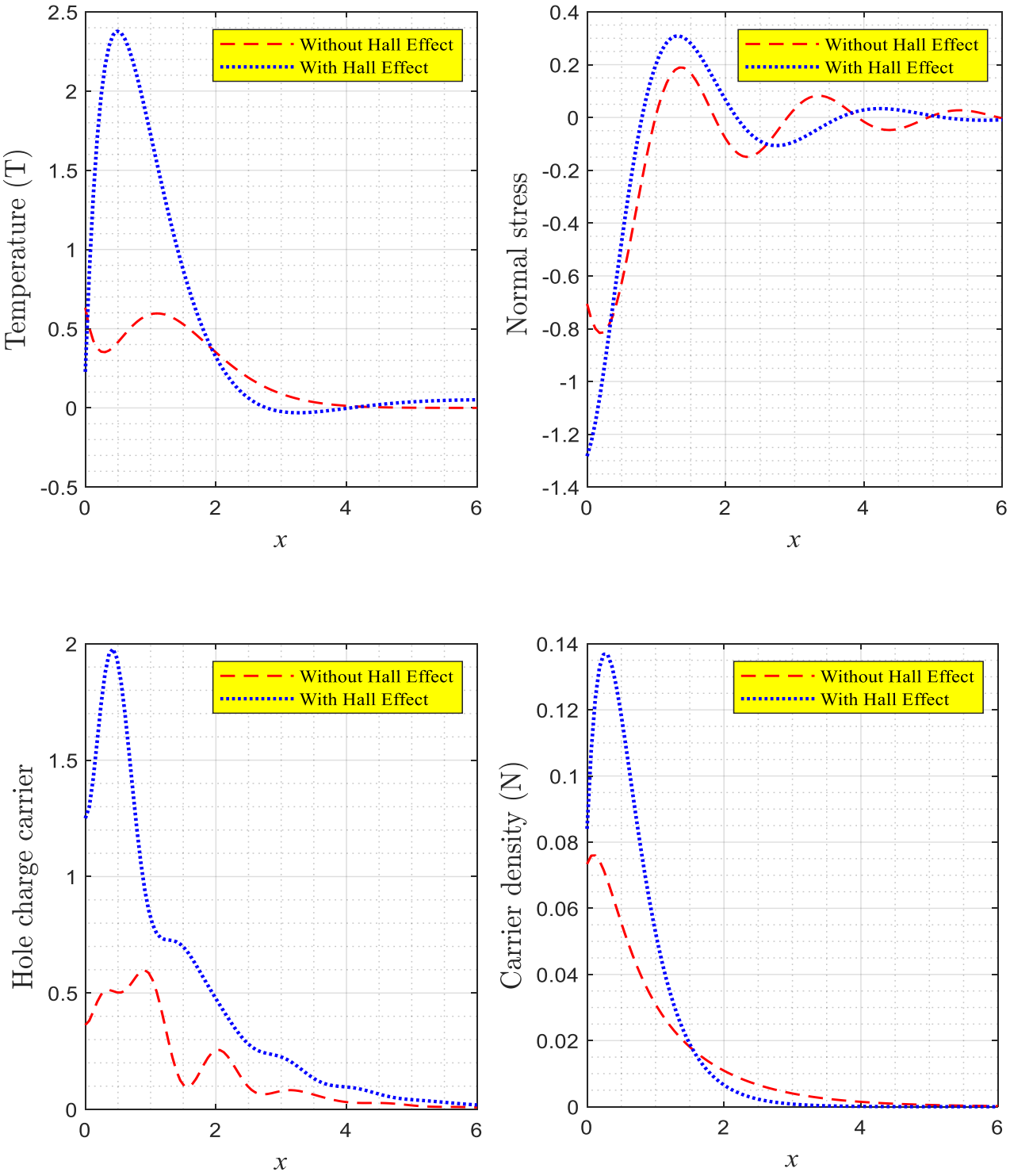


Figure 4. The DPL model's change of non-local physical fields along with changing thermal conductivity in the absence and presence of Hall current.

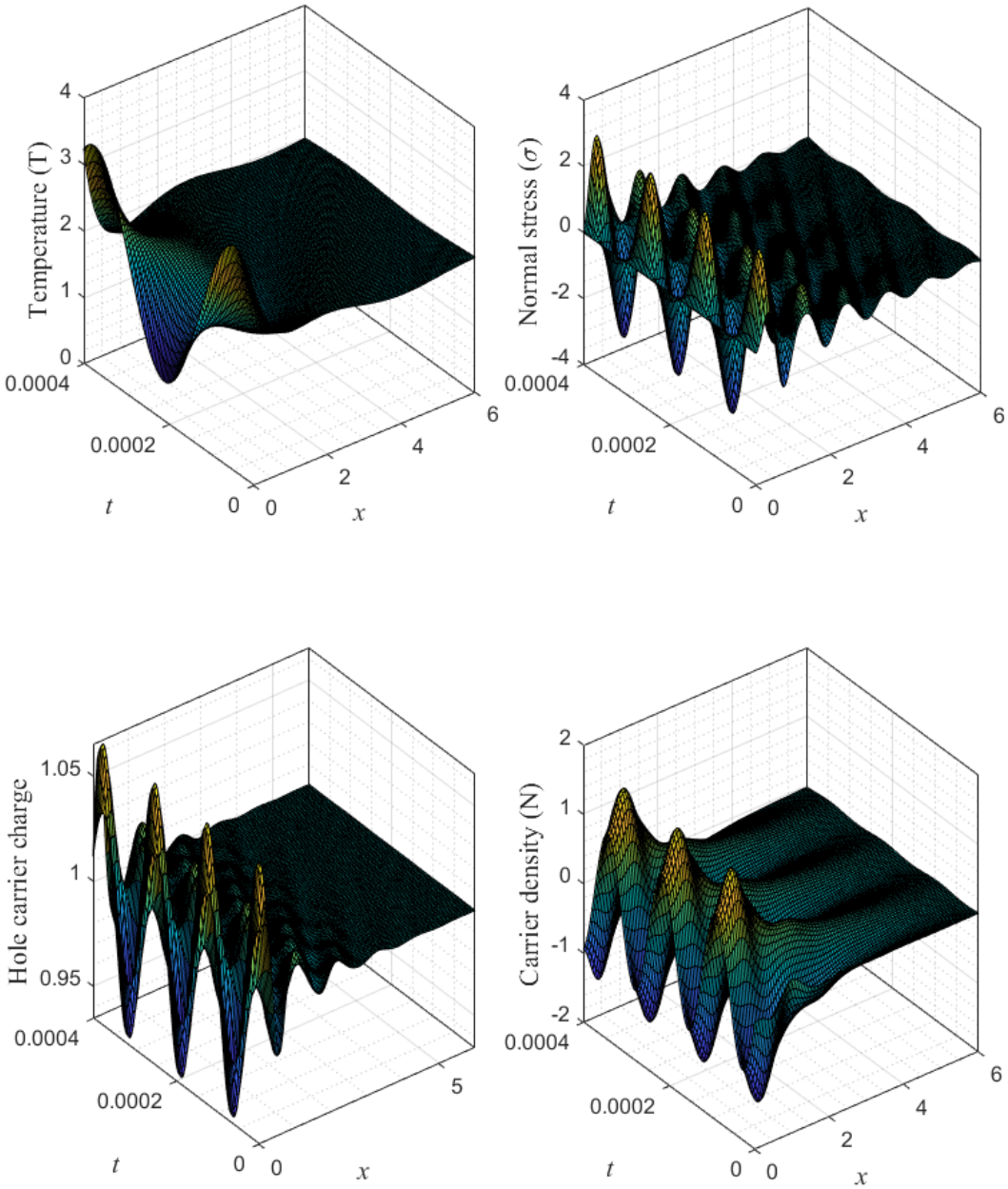


Figure 5. According to the DPL model, the 3D main field distributions change with distance and time when variable thermal conductivity and Hall current are at play.

7.3. The Impact of Hall Current

The third group (Figure 4) shows how the Hall current, which is connected to a strong magnetic field, affects physical fields and distributions as axial distance x increases. When the non-local semiconductor medium ($\xi_1 = 0.50$) depends on temperature ($K_\theta = -0.4$), all numerical computations are performed for short periods of time in accordance with the DPL model. When the impact of the strong magnetic field is disregarded, the impact of the Hall current is also disregarded in the first example (the Hartmann number is removed). The influence of the Hall current brought on by the presence of the magnetic field is explored in the second scenario. As demonstrated by this group's research, the interior particles of semiconductors are rearranged by the strong magnetic field (Hall current), and this is evident in all physical quantity distributions, particularly the hole charge carrier distribution [38–43].

7.4. The 3D Graph

Figure 5 shows three-dimensional (3D) graphs under the impact of varying thermal conductivity and a high magnetic field, and with the Hall current effect according to the DPL model for Si media. This diagram examines the variations in the wave distribution of basic physical parameters in relation to changes in both time and distance. The dimensionless time interval $0 \leq t \leq 4 \times 10^{-4}$ can be obtained when, regarding this figure, time variation affects the propagation of waves in all boundary-constrained physical domains. The size of the wave propagations in all physical domains is, however, influenced by the axial distance and time scale disparities. As distance and time increase, all wave propagation vanishes and moves closer to the zero line, as predicted by the steady-state.

8. Conclusions

In this work, the interaction between electrons and holes is considered, and a novel model for the coupling of the thermoelastic and plasma waves in 1D deformation of non-local semiconductor medium is examined. The effect of a magnetic field, which occurs along with the effect of Hall current when the medium is temperature-dependent, was studied in relation to the novel model. Due to the intricacy of the concept, only a small number of reviews of the literature for this model have been published where the coupling between holes and electrons, Hall current effect, and changing thermal conductivity are taken into account. Fourier's law and diffusion typically provide an easier and better description in engineering applications, but if the relaxation and process times are comparable, it would be desirable to take both diffusion and relaxation into account by using constitutive models that include both thermal conductivity and relaxation time. The analysis of this model makes it abundantly evident that the Hall current effect, the changing in thermal conductivity, space–time, and variations in thermal relaxation times all significantly impact how waves propagate for all physical fields in the non-local semiconductor medium. In fact, the physical characteristics of some materials, particularly non-local semiconducting materials, can alter due to variations in the magnetic field and thermal conductivity. When studying elastic non-local semiconductor media, particularly the Hall sensor, Hall potentiometer, and electronics technology, the studies of Hall current and variable thermal conductivity can be quite helpful to scientists.

Author Contributions: M.H.R.: methodology, software; K.L.: validation, formal analysis; A.A.: investigation, resources; R.C.: data curation; A.A.E.-B.: writing—review and editing; A.M.: visualization, supervision. All authors have read and agreed to the published version of the manuscript.

Funding: This research received no external funding.

Institutional Review Board Statement: Not applicable.

Informed Consent Statement: Not applicable.

Data Availability Statement: The datasets used and/or analyzed during the current study are available from the corresponding author on reasonable request.

Conflicts of Interest: The authors declare no conflict of interest.

Nomenclature (The Physical Quantities with Units)

λ, μ	**Elastic Lame's Parameters**
$\delta_n = (3\lambda + 2\mu)d_n$	Deformation potential difference between conduction and valence band
d_n	Electronic deformation coefficient ED
T_0	Reference temperature in its natural state
$\gamma = (3\lambda + 2\mu)\alpha_t$	Volume thermal expansion

σ_{ij}	Stress tensor
ρ	Density of the sample
α_t	Linear thermal expansion
n_0	Equilibrium carrier concentration
C_e	Specific heat at constant strain
K	Thermal conductivity of the semiconductor medium
t^n, t^h	Electrons and holes relaxation times
t_1^n	Lifetime of photogenerated carriers
E_g	Energy gap
e_{ij}	Components of the strain tensor
$m_{nq}, m_{qn}, m_{hq}, m_{qh}$	Peltier–Seebeck–Dufour–Soret-like constants
$a_{Qn}, a_{Qh}, a_Q, a_n,\ a_h$	Flux-like constants
τ_θ, τ_q	Thermal and elastic relaxation times
α_h, α_n	Holes and electrons thermo-diffusive parameters
h_0	Equilibrium holes concentration
$\delta_h = (2\mu + 3\lambda)d_h$	Holes elastodiffusive parameter
d_h	Coefficients of hole deformation
$\widetilde{s}$	Recombination velocities
D_n, D_h	Diffusion coefficients of electrons and holes

Appendix A

The main coefficients of the Equation (33) can be obtained with the helping of software computer programming, and take the following form:

$$\left.\begin{array}{l} \prod_1 = \frac{-1}{(\alpha_9\alpha_{14}q_1-\alpha_1\alpha_{14}-\alpha_5\alpha_9)}(\alpha_{14}q_1(\Upsilon\alpha_9-\alpha_1q_{14})+\alpha_9q_{14}(\alpha_5q_{13} \\ +\alpha_{14}q_5)+\alpha_{21}\alpha_9q_{13}q_1-\alpha_1\alpha_{14}(\Upsilon+q_7)-\alpha_1\alpha_{21}q_9-\alpha_9q_4- \\ \alpha_1\alpha_{21}q_{13}-\alpha_5\alpha_9q_{10}+\alpha_{14}\alpha_9q_2-\alpha_9\alpha_{21}q_5+\alpha_9q_1q_{11}+\alpha_{14}q_1q_6+ \\ q_6(\alpha_{14}q_1-\alpha_5)-\alpha_1(q_{11}-q_8)+\alpha_5(q_{12}+q_{13})-\alpha_{14}(q_3+q_5)) \end{array}\right\} \quad \text{(A1)}$$

$$\left.\begin{array}{l} \prod_2 = \frac{1}{(\alpha_9\alpha_{14}q_1-\alpha_1\alpha_{14}-\alpha_5\alpha_9)}\Upsilon(\alpha_9\alpha_{14}q_1+\alpha_9(\alpha_5q_{10}-\alpha_{14}q_2-q_1q_{11}) \\ -\alpha_{14}q_1q_6)+\alpha_1(\alpha_{21}q_7q_{13}-\alpha_{21}q_9q_{10}-q_{14}(q_8q_{13}-q_9q_{11}))+\alpha_5q_{14}(q_6q_{13}- \\ q_9q_{12})-\alpha_9\alpha_{21}(q_2q_{13}-q_5q_{10})+\alpha_9q_{14}(q_4q_{13}-q_5q_{11})+\alpha_{14}q_{14}(q_3q_9-q_5q_6)- \\ \alpha_{21}q_1(q_6q_{13}+q_9q_{12})-\Upsilon(\alpha_1(q_8-q_{11})+\alpha_5q_{12}-\alpha_9q_4-\alpha_{14}q_3)+\alpha_1(q_7q_{11}- \\ q_8q_{10})+\alpha_5(q_6q_{10}-q_7(q_{12}+q_{13})+q_9q_{10})-\alpha_9(q_2q_{11}-q_4q_{10})- \\ \alpha_{14}q_2(q_6-q_9)-q_7(q_3+q_7)-\alpha_{21}^*(q_3q_{13}-q_5(q_6+q_{12}))-\alpha_{21}q_1(q_6q_{11}- \\ q_8(q_{12}+q_{13})+q_9q_{11})-q_3(q_8-q_{11})+q_4(q_6+q_9-q_{12}+q_{13})-q_5(q_8-q_{11}) \end{array}\right\} \quad \text{(A2)}$$

$$\left.\begin{array}{l} \prod_3 = \frac{-1}{(\alpha_9\alpha_{14}q_1-\alpha_1\alpha_{14}-\alpha_5\alpha_9)}\{\Upsilon(\alpha_1q_8q_{10}-\alpha_1q_7q_{11}-\alpha_5q_6q_{10} \\ +\alpha_5q_7q_{12}+\alpha_9(q_2q_{11}-q_4q_{10})+\alpha_{14}(q_2q_6-q_3q_7)+q_1(q_6q_{11}-q_8q_{12}))+ \\ +\alpha_{21}(q_2(q_6q_{13}-q_9q_{12})-q_3(q_7q_{13}-q_9q_{10})-q_5(q_6q_{10}-q_7q_{12}))+ \\ q_3q_{14}(q_8q_{13}-q_9q_{11})-q_4q_{14}(q_6q_{13}-q_9q_{12})-q_5q_{14}(q_6q_{11}-q_8q_{12})+\Upsilon(\\ q_3(q_8-q_{11})-q_4(q_6-q_{12}))+q_2(q_6q_{11}-q_8q_{12}-q_8q_{13}+q_9q_{11})-\alpha_{21}q_3(q_7q_{11}- \\ q_8q_{10})-q_4(q_6q_{10}-q_7(q_{12}+q_{13})+q_9q_{10})+\alpha_{21}q_5(q_8q_{10}-q_8q_{10})\} \end{array}\right\} \quad \text{(A3)}$$

$$\left.\prod_4 = \frac{\Upsilon(-q_2q_6q_{11}+q_2q_8q_{12}+q_3\alpha_{21}(q_7q_{11}-q_8q_{10})+q_4\alpha_{21}(q_6q_{10}-q_7q_{12}))}{(-\alpha_9\alpha_{14}q_1+\alpha_1\alpha_{14}+\alpha_5\alpha_9)}\right\} \quad \text{(A4)}$$

On the other hand, the coefficients of the Equation (40) are:

$$\left.\begin{aligned}
c_1 &= \alpha_9(-q_{13}q_{14} - R_H - q_{10}) - q_6 - q_9 + q_{12} + q_{13}\\
c_2 &= R_H\alpha_9 q_{10} + q_9 q_{13} q_{14} - q_9 q_{12} q_{14} + R_H(q_6 - q_{12}) + q_6 q_{10} - q_7 q_{12} - q_7 q_{13} + q_9 q_{10}\\
c_3 &= R_H(-q_6 q_{10} + q_7 q_{12})\\
c_4 &= -R_H\alpha_9\alpha_{14} - \alpha_9\alpha_{21}q_{13} - \alpha_9 q_{11} - \alpha_{14}q_6 - \alpha_{14}q_9\\
c_5 &= R_H\alpha_9 q_{11} + R_H\alpha_{14}q_6 + \alpha_{21}q_6 q_{13} - \alpha_{21}q_9 q_{12} + q_6 q_{11} - q_8 q_{12} - q_8 q_{13} + q_9 q_{11}\\
c_6 &= R_H(-q_6 q_{11} + q_8 q_{12})\\
c_7 &= \alpha_{14}(-q_9 q_{14} - R_H - q_7) + \alpha_{21}(q_9 - q_{13}) + q_8 - q_{11}\\
c_8 &= R_H\alpha_{14}q_7 + \alpha_{21}(q_7 q_{13} - q_9 q_{10}) - q_8 q_{13} q_{14} + q_9 q_{11} q_{14} - R_H(q_8 - q_{11}) + q_7 q_{11} - q_8 q_{10}\\
c_9 &= R_H(-q_7 q_{11} + q_8 q_{10})\\
c_{10} &= \alpha_9(\alpha_{14}q_{14} - \alpha_{21} - \alpha_{14})\\
c_{11} &= \alpha_9\alpha_{21}q_{10} + \alpha_9 q_{11} q_{14} - \alpha_{14}q_6 q_{14} - q_8 q_{12} q_{14} + \alpha_{14}q_7 + \alpha_{21}(q_6 - q_{12}) - q_8 + q_{11}\\
c_{12} &= -\alpha_{21}q_6 q_{10} + \alpha_{21}q_7 q_{12} + q_6 q_{11} q_{14} - q_8 q_{12} q_{14} - q_7 q_{11} + q_8 q_{10}
\end{aligned}\right\} \quad \text{(A5)}$$

References

1. Todorovic, D. Plasma, thermal, and elastic waves in semiconductors. *Rev. Sci. Instrum.* **2003**, *74*, 582–585. [CrossRef]
2. Hall, E.H. On a New Action of the Magnet on Electric Currents. *Am. J. Math.* **1879**, *2*, 287–292. [CrossRef]
3. Biot, M.A. Thermoelasticity and irreversible thermodynamics. *J. Appl. Phys.* **1956**, *27*, 240–253. [CrossRef]
4. Lord, H.; Shulman, Y.A. Generalized dynamical theory of Thermoelasticity. *J. Mech. Phys. Solids* **1967**, *15*, 299–309. [CrossRef]
5. Green, A.E.; Lindsay, K.A. Thermoelasticity. *J. Elast.* **1972**, *2*, 1–7. [CrossRef]
6. Chandrasekharaiah, D.S. Thermoelasticity with second sound: A review. *Appl. Mech. Rev.* **1986**, *39*, 355–376. [CrossRef]
7. Chandrasekharaiah, D.S. Hyperbolic Thermoelasticity: A review of recent literature. *Appl. Mech. Rev.* **1998**, *51*, 705–729. [CrossRef]
8. Sharma, J.N.; Kumar, V.; Dayal, C. Reflection of generalized thermoelastic waves from the boundary of a half-space. *J. Therm. Stress.* **2003**, *26*, 925–942. [CrossRef]
9. Lotfy, K.; Abo-Dahab, S. Two-dimensional problem of two temperature generalized thermoelasticity with normal mode analysis undethermal shock problem. *J. Comput. Theor. Nanosci.* **2015**, *12*, 1709–1719. [CrossRef]
10. Othman, M.; Lotfy, K. The influence of gravity on 2-D problem of two temperature generalized thermoelastic medium with thermal relaxation. *J. Comput. Theor. Nanosci.* **2015**, *12*, 2587–2600. [CrossRef]
11. Maruszewski, B. Electro-magneto-thermo-elasticity of Extrinsic Semiconductors, Classical Irreversible Thermodynamic Approach. *Arch. Mech.* **1986**, *38*, 71–82.
12. Maruszewski, B. Electro-magneto-thermo-elasticity of Extrinsic Semiconductors, Extended Irreversible Thermodynamic Approach. *Arch. Mech.* **1986**, *38*, 83–95.
13. Maruszewski, B. Coupled Evolution Equations of Deformable Semiconductors. *Int. J. Eng. Sci.* **1987**, *25*, 145–153. [CrossRef]
14. Sharma, J.N.; Thakur, N.T. Plane harmonic elasto-thermodiffusive waves in semiconductor materials. *J. Mech. Mater. Struct.* **2006**, *1*, 813–835. [CrossRef]
15. Mandelis, A. *Photoacoustic and Thermal Wave Phenomena in Semiconductors*; Elsevier: New York, NY, USA, 1987.
16. Almond, D.; Patel, P. *Photothermal Science and Techniques*; Springer Science & Business Media: Berlin/Heidelberg, Germany, 1996.
17. Gordon, J.P.; Leite, R.C.C.; Moore, R.S.; Porto, S.P.S.; Whinnery, J.R. Long-transient effects in lasers with inserted liquid samples. *Bull. Am. Phys. Soc.* **1964**, *119*, 3–8. [CrossRef]
18. Lotfy, K. Effect of variable thermal conductivity during the photothermal diffusion process of semiconductor medium. *Silicon* **2019**, *11*, 1863–1873. [CrossRef]
19. Todorovic, D.M.; Nikolic, P.M.; Bojicic, A.I. Photoacoustic frequency transmission technique: Electronic deformation mechanism in semiconductors. *J. Appl. Phys.* **1999**, *85*, 7716–7726. [CrossRef]
20. Tam, A.C. Applications of photoacoustic sensing techniques. *Rev. Mod. Phys.* **1986**, *58*, 381. [CrossRef]
21. Lotfy, K.; El-Bary, A.A.; Hassan, W.; Ahmed, M.H. Hall current influence of microtemperature magneto-elastic semiconductor material. *Superlattices Microstruct.* **2020**, *139*, 106428. [CrossRef]
22. Mahdy, A.M.S.; Lotfy, K.; Ahmed, M.H.; El-Bary, A.; Ismail, E.A. Electromagnetic Hall current effect and fractional heat order for microtemperature photo-excited semiconductor medium with laser pulses. *Results Phys.* **2020**, *17*, 103161. [CrossRef]
23. Mahdy, A.M.S.; Lotfy, K.; El-Bary, A.; Tayel, I.M. Variable thermal conductivity and hyperbolic two-temperature theory during magneto-photothermal theory of semiconductor induced by laser pulses. *Eur. Phys. J. Plus* **2021**, *136*, 651. [CrossRef]
24. Hosseini, S.; Sladek, J.; Sladek, V. Application of meshless local integral equations to two-dimensional analysis of coupled non-Fick diffusion elasticity. *Eng. Anal. Bound. Elem.* **2013**, *37*, 603–615. [CrossRef]

25. Lotfy, K. A Novel Model of Photothermal Diffusion (PTD) fo Polymer Nano- composite Semiconducting of Thin Circular Plate. *Phys. B Condens. Matter* **2018**, *537*, 320–328. [CrossRef]
26. Lotfy, K.; Hassan, W.; Gabr, M. Thermomagnetic effect with two temperature theory for photothermal process under hydrostatic initial stress. *Results Phys.* **2017**, *7*, 3918–3927. [CrossRef]
27. Yadav, A. Photothermal plasma wave in the theory of two-temperature with multi-phase-lag thermo-elasticity in the presence of magnetic field in a semiconductor with diffusion. *Waves Random Complex Media* **2022**, *32*, 2416–2444. [CrossRef]
28. Lotfy, K. A novel model for Photothermal excitation of variable thermal conductivity semiconductor elastic medium subjected to mechanical ramp type with two-temperature theory and magnetic field. *Sci. Rep.* **2019**, *9*, 3319. [CrossRef] [PubMed]
29. Zhou, H.; Shao, D.; Li, P. Thermoelastic damping and frequency shift in micro/nano-ring resonators considering the nonlocal single-phase-lag effect in the thermal field. *Appl. Math. Model.* **2023**, *115*, 237–258. [CrossRef]
30. Lata, P.; Singh, S. Effects of Hall current and nonlocality in a magneto-thermoelastic solid with fractional order heat transfer due to normal load. *J. Therm. Stress.* **2022**, *45*, 51–64. [CrossRef]
31. Honig, G.; Hirdes, U. A method for the numerical inversion of LaplaceTransforms, Comp. *Appl. Math.* **1984**, *10*, 113–132.
32. Marin, M. A partition of energy in thermoelasticity of microstretch bodies. *Nonlinear Anal. Real World Appl.* **2010**, *11*, 2436–2447. [CrossRef]
33. Abbas, I.; Marin, M. Analytical Solutions of a Two-Dimensional Generalized Thermoelastic Diffusions Problem Due toLaser Pulse. *Iran. J. Sci. Technol. Trans. Mech. Eng.* **2018**, *42*, 57–71. [CrossRef]
34. Mondal, S.; Sur, A. Photo-thermo-elastic wave propagation in anorthotropic semiconductor with a spherical cavity and memory responses. *Wavesin Random Complex Media* **2021**, *31*, 1835–1858. [CrossRef]
35. El-Sapa, S.; Lotfy, K.; El-Bary, A. The Hall current effect of magnetic-optical-elastic-thermal-diffusive semiconductor model during electrons-holes excitation processes. *Waves Random Complex Media* **2022**. [CrossRef]
36. Mustafa, F.; Hashim, A.M. Plasma Wave Electronics: A Revival Towards Solid-State Terahertz Electron Devices. *J. Appl. Sci.* **2010**, *10*, 1352–1368. [CrossRef]
37. Brancik, L. Programs for fast numerical inversion of Laplace transforms in MATLAB language environment. In Proceedings of the 7th Conference MATLAB, Prague, Czech Republic, 3 November 1999; Volume 99, pp. 27–99.
38. Alhejaili, W.; Lotfy, K.; El-Bary, A. Photo–elasto–thermodiffusion waves of semiconductor with ramp-type heating for electrons–holes-coupled model with initial stress. *Waves Random Complex Media* **2022**, 1–19. [CrossRef]
39. Abbas, I.A. A GN model for thermoelastic interaction in an unbounded fiber-reinforced anisotropic medium with a circular hole. *Appl. Math. Lett.* **2013**, *26*, 232–239. [CrossRef]
40. Abbas, I.A. Eigenvalue approach on fractional order theory of thermoelastic diffusion problem for an infinite elastic medium with a spherical cavity. *Appl. Math. Model.* **2015**, *39*, 6196–6206. [CrossRef]
41. Abbas, I.A.; Abdalla, A.-E.N.N.; Alzahrani, F.S.; Spagnuolo, M. Wave propagation in a generalized thermoelastic plate using eigenvalue approach. *J. Therm. Stress.* **2016**, *39*, 1367–1377. [CrossRef]
42. Abbas, I.A. Analytical solution for a free vibration of a thermoelastic hollow sphere. *Mech. Based Des. Struct. Mach.* **2015**, *43*, 265–276. [CrossRef]
43. Abbas, I.A.; Alzahranib, F.S.; Elaiwb, A. A DPL model of photothermal interaction in a semiconductor material. *Waves Random Complex Media* **2019**, *29*, 328–343. [CrossRef]
44. Xiao, Y.; Shen, C.; Zhang, W.B. Screening and prediction of metal-doped α-borophene monolayer for nitric oxide elimination. *Mater. Today Chem.* **2022**, *25*, 100958. [CrossRef]
45. Liu, J.; Han, M.; Wang, R.; Xu, S.; Wang, X. Photothermal phenomenon: Extended ideas for thermophysical properties characterization. *J. Appl. Phys.* **2022**, *131*, 065107. [CrossRef]

Disclaimer/Publisher's Note: The statements, opinions and data contained in all publications are solely those of the individual author(s) and contributor(s) and not of MDPI and/or the editor(s). MDPI and/or the editor(s) disclaim responsibility for any injury to people or property resulting from any ideas, methods, instructions or products referred to in the content.